JOURNAL OF BACTERIOLOGY, Nov. 2006, p. 7731–7741 Vol. 188, No. 22
0021-9193/06/$08.00+0 doi:10.1128/JB.00761-06

Interaction between Coat Morphogenetic Proteins SafA and SpoVID▽

Teresa Costa,[1]† Anabela L. Isidro,[1] Charles P. Moran, Jr.,[2] and Adriano O. Henriques[1]*

Instituto de Tecnologia Química e Biológica, Universidade Nova de Lisboa, Avenida da República, EAN, 2781-157 Oeiras, Portugal,[1] and Emory University School of Medicine, Department of Microbiology and Immunology, 3010 Rollins Research Center, Atlanta, Georgia 30322[2]

Received 26 May 2006/Accepted 23 August 2006

Morphogenetic proteins such as SpoVID and SafA govern assembly of the *Bacillus subtilis* endospore coat by guiding the various protein structural components to the surface of the developing spore. Previously, a screen for peptides able to interact with SpoVID led to the identification of a PYYH motif present in the C-terminal half of the SafA protein and to the subsequent demonstration that SpoVID and SafA directly interact. *spoVID* and *safA* spores show deficiencies in coat assembly and are lysozyme susceptible. Both proteins, orthologs of which are found in all *Bacillus* species, have LysM domains for peptidoglycan binding and localize to the cortex-coat interface. Here, we show that the interaction between SafA and SpoVID involves the PYYH motif (region B) but also a 13-amino-acid region (region A) just downstream of the N-terminal LysM domain of SafA. We show that deletion of region B does not block the interaction of SafA with SpoVID, nor does it bring about spore susceptibility to lysozyme. Nevertheless, it appears to reduce the interaction and affects the complex. In contrast, lesions in region A impaired the interaction of SafA with SpoVID in vitro and, while not affecting the accumulation of SafA in vivo, interfered with the localization of SafA around the developing spore, causing aberrant assembly of the coat and lysozyme sensitivity. A peptide corresponding to region A interacts with SpoVID, suggesting that residues within this region directly contact SpoVID. Since region A is highly conserved among SafA orthologs, this motif may be an important determinant of coat assembly in the group of *Bacillus* spore formers.

A large number of proteins produced in the mother cell of sporulating cells of *Bacillus subtilis* are targeted to the surface of the developing spore to form a structure known as the spore coat (11, 16, 18). Assembly of the coat confers protection against lytic enzymes and small noxious molecules and allows efficient interaction of the spore with compounds able to trigger germination (11, 16, 18). Because of the resistance it imparts to the action of the lytic enzymes, the coat also protects phagocytosed spores from digestion by predatory microorganisms (22). Structurally, the coat consists of an amorphous undercoat that contacts the underlying cortex peptidoglycan, a lamellar inner layer, and a thick electron-dense outer layer (11, 16, 18). The genes encoding the various coat components are expressed at different times during the deployment of a mother cell cascade of gene expression, and this temporal control is an important factor contributing to the ordered assembly of the coat (16). However, assembly of the coat relies to a large extent on the action of a class of so-called morphogenetic proteins that guide the assembly of the structural components (11, 16, 18, 29). One, called SpoIVA, localizes early to the mother cell side of the asymmetric septum and is responsible for recruiting another morphogenetic protein, SpoVID, to the developing spore (11, 12, 33). A third morphogenetic protein, CotE, localizes in a SpoIVA-dependent manner close to the developing spore, around a region of unknown composition called the matrix (11, 12). The localizations of SpoIVA, SpoVID, and CotE take place prior to the complete engulfment of the prespore by the mother cell when σ^E and the ancillary transcription factors SpoIIID and GerR govern gene expression in the mother cell (13, 41). Following engulfment completion, and the activation of the late mother cell-specific regulators σ^K and later of GerE, the coat layers start gaining their final appearance (11, 13, 16, 18, 41). The prior localization of CotE at the edge of the matrix region is thought to be required to nucleate assembly of the outer coat, whereas the matrix region develops into the inner coat (11, 12). CotE appears to have a modular design, specifying information for its targeting to the surface of the developing spore, for oligomerization, and also for interaction with other coat proteins (3, 28). Presumably, CotE controls outer coat assembly by means of complex network of direct or indirect interactions leading to the recruitment of many proteins to this coat layer (21, 28).

SpoVID does not influence the localization of CotE at an early stage, but following engulfment completion in cells mutant for *spoVID*, CotE and the rest of the coat detaches from the surface of the prespore and forms swirls of partially structured material dispersed throughout the mother cell cytoplasm (4, 12). Left with an exposed cortex, *spoVID* spores are sensitive to lysozyme (12). To study the function of SpoVID in the assembly process, Ozin et al. (32) used a phage display screening to identify peptides able to interact with SpoVID. They found a peptide motif, PYYH, occurring in the C-terminal half of another coat protein, SafA (387 residues long), the absence of which causes deficient formation of the coat and spore susceptibility to lysozyme (32, 40). At least three forms of SafA accumulate in sporulating cells: a full-length form ($SafA_{FL}$) (45

* Corresponding author. Mailing address: Instituto de Tecnologia Química e Biológica, Universidade Nova de Lisboa, Avenida da República, EAN, 2781-157 Oeiras, Portugal. Phone: 351-21-4469522. Fax: 351-21-4411277. E-mail: aoh@itqb.unl.pt.

† Present address: Department of Molecular, Cellular, and Developmental Biology, Yale University, New Haven, CT 06520.

▽ Published ahead of print on 1 September 2006.

TABLE 1. Bacterial strains used in this study

Strain	Genotype/phenotype[a]	Origin or reference
E. coli strains		
CC118	(DE3)/pLysS	Colin Manoil
AH2687	CC118(DE3)/pLysS/pTC55 Cm^r Amp^r	This work
AH2688	CC118(DE3)/pLysS/pTC49 Cm^r Amp^r	This work
AH2689	CC118(DE3)/pLysS/pTC50 Cm^r Amp^r	This work
AH2690	CC118(DE3)/pLysS/pTC51 Cm^r Amp^r	This work
AH2691	CC118(DE3)/pLysS/pTC52 Cm^r Amp^r	This work
AH2718	CC118(DE3)/pLysS/pTC61 Cm^r Amp^r	This work
AH2719	CC118(DE3)/pLysS/pTC62 Cm^r Amp^r	This work
AH2692	CC118(DE3)/pLysS/pOZ169 Cm^r Amp^r	This work
AH2934	CC118(DE3)/pLysS/pTC138 Cm^r Amp^r	This work
AH2935	CC118(DE3)/pLysS/pTC139 Cm^r Amp^r	This work
AH2937	CC118(DE3)/pLysS/pTC141 Cm^r Amp^r	This work
AH2978	CC118(DE3)/pLysS/pTC159 Cm^r Amp^r	This work
AH2979	CC118(DE3)/pLysS/pTC160 Cm^r Amp^r	This work
AH2980	CC118(DE3)/pLysS/pTC161 Cm^r Amp^r	This work
AH2985	CC118(DE3)/pLysS/pTC165 Cm^r Amp^r	This work
AH4086	CC118(DE3)/pLysS/pTC196 Cm^r Amp^r	This work
AH4087	CC118(DE3)/pLysS/pTC197 Cm^r Amp^r	This work
B. subtilis strains		
AOB68	*trpC2 metC3* Δ*safA*::*sp* Sp^r	32
AOB90	*trpC2 metC3 safA-flag* Cm^r	33
AH2781	*trpC2 metC3* Δ*safA*::$safA_{\Delta PYYH}$ Sp^r Cm^r	This work
AH2787	*trpC2 metC3* Δ*safA*::$safA_{N1–162}$ Sp^r Cm^r	This work
AH2788	*trpC2 metC3* Δ*safA*::$safA_{C164–387}$ Sp^r Cm^r	This work
AH4006	*trpC2 metC3* Δ*safA*::$safA_{\Delta G51-S63}$ Sp^r Cm^r	This work
AH4090	*trpC2 metC3* Δ*safA*::$safA_{\Delta G51-E57}$ Sp^r Cm^r	This work
AH4091	*trpC2 metC3* Δ*safA*::$safA_{\Delta P58-S63}$ Sp^r Cm^r	This work
AH4007	*trpC2 metC3* Δ*safA*::$safA_{4\times Ala}$ Sp^r Cm^r	This work
AH4102	*trpC2 metC3* Δ*safA*::$safA^+$-*gfp* Sp^r Nm^r	This work
AH4103	*trpC2 metC3* Δ*safA*::$safA_{\Delta G51-S63}$-*gfp* Sp^r Nm^r	This work
AH4107	*trpC2 metC3* Δ*spoVID*::*cm* Δ*safA*::$safA^+$-*gfp* Sp^r Cm^r Nm^r	This work
AH4108	*trpC2 metC3* Δ*spoVID*::*cm* Δ*safA*::$safA_{\Delta G51-S63}$-*gfp* Sp^r Cm^r Nm^r	This work

[a] Sp^r, spectinomycin resistant; Cm^r, chloramphenicol resistant; Nm^r, neomycin resistant.

kDa), a C-terminal form derived from internal translation of the *safA* mRNA at methionine 164 ($SafA_{C30}$, 30 kDa) and an N-terminal form ($SafA_{N21}$, 21 kDa) (31). Assays in vitro and in vivo showed that SafA and SpoVID directly interact, that SafA interacts with itself, and that each of the C- and N-terminal forms are capable of interacting with $SafA_{FL}$, with themselves, and, for at least $SafA_{N21}$, with SpoVID (33). Both SpoVID (at its C terminus) and SafA (at its N terminus) contain a LysM domain, which has a general peptidoglycan-binding function (2, 5, 20, 27, 35, 39), and both proteins localize to the cortex/coat interface (12, 32). Moreover, the localization of SafA depends on SpoVID (33). These results have led to a model according to which the interaction between SafA and SpoVID recruits the former to the coat region in close proximity to the cortex layer, and the two proteins function in this region by promoting attachment of the nascent coat to the underlying cortex layer (33). However, in spite of the fact that it contains the PYYH motif, the $SafA_{C30}$ form is not recruited to the prespore in the absence of $SafA_{FL}$, suggesting that a second region of interaction could exist in the N-terminal half of SafA (33). This second region of interaction between SafA and SpoVID was attributed to the LysM domain of both proteins, which is presumed to be involved in multimerization (2, 5, 20, 27, 35).

Here, we have analyzed the interaction between SafA and SpoVID. We present biochemical, cytological, and genetic evidence that strongly suggests that the interaction of SafA with SpoVID via a region just downstream of the LysM domain is responsible for the targeting of SafA to the surface of the developing spore and for the proper assembly and function of the coat structure.

MATERIALS AND METHODS

Strains and general techniques. All of the *B. subtilis* strains used in this study are congenic derivatives of the wild-type strain MB24 (*trpC2 metC3*) (Table 1). The *Escherichia coli* strain DH5α (Bethesda Research Laboratories) was used for molecular cloning, and CC118(DE3)/pLysS was used for the overproduction of native or glutathione *S*-transferase (GST) fusion proteins (Table 1). Luria-Bertani medium was used for maintenance and growth of *E. coli* and *B. subtilis* strains, with appropriate antibiotic selection when needed. Sporulation was induced by growth and nutrient exhaustion in Difco sporulation medium (DSM) (30). Genetic manipulations of *B. subtilis* and spore resistance or germination properties were assessed as previously described (9).

GST-SafA fusions. Primer *safA*204D and primer *safA*-STOP51R, *safA*-STOP64R, *safA*-STOP78R, *safA*-STOP91R, or *safA*-STOP99R (the sequences of all primers are available upon request) were used to PCR amplify the coding regions of *safA* from residues 1 to 50, 1 to 63, 1 to 77, 1 to 90, and 1 to 98, respectively. The PCR fragments were digested with BamHI and XhoI and cloned between the same sites of pGex4T-3 (Pharmacia) to form pTC138 (GST-$SafA_{E50}$), pTC159 (GST-$SafA_{S63}$), pTC160 (GST-$SafA_{K77}$), pTC161 (GST-$SafA_{K90}$), and pTC139 (GST-$SafA_{P98}$), respectively. The region encompassing codons 1 to 162 of *safA* was amplified with primers *safA*204D and *safA*693R, digested with BamHI, and cloned between the BamHI site and a filled-in XhoI site of pGex4T-3 (Pharmacia) to yield pTC141 (GST-$SafA_{S162}$). pTC165 (GST-$SafA_{\Delta G51-S63}$) was obtained after digestion with HincII and autoligation of a

PCR obtained from pTC139 (see above) with primers *safA*50-64D and *safA*50-64R. pTC196 (GST-SafA$_{\Delta G51\text{-}E57}$) and pTC197 (GST-SafA$_{\Delta P58\text{-}S63}$) were constructed as follows. First, the *safA* coding regions from residues 1 to 50 and 1 to 57 were PCR amplified with primer sets *safA*204D/*safA*51-57R and *safA*204D/*safA*58-63R, respectively. Second, the regions corresponding to residues 58 to 98 and 64 to 98 of *safA* were PCR amplified with primer sets *safA*51-57D/*safA*-STOP99R and *safA*58-63D/*safA*-STOP99R, respectively. The fragments (codons 1 to 50 and 58 to 98 or 1 to 57 and 64 to 98) were mixed and subjected to PCR using primers *safA*204D and *safA*-STOP99R to obtain *safA* fragments comprising the region coding for the first 98 residues but excluding residues 51 to 57 or 58 to 63, respectively. The fragments were digested with BamHI and XhoI and introduced between identical sites of pGex4T-3 (Pharmacia) to create pTC196 and pTC197. All PCR products were sequenced. Plasmids pTC138, pTC159, pTC160, pTC161, pTC139, pTC141, pTC165, pTC196, and pTC197 were used to transform *E. coli* CC118(DE3)/pLysS to obtain strains AH2934, AH2978, AH2979, AH2980, AH2935, AH2937, AH2985, AH4086, and AH4087, respectively (Table 1).

GST-SpoVID fusions. Strain AH2692 (Table 1) was obtained by transformation of *E. coli* CC118(DE3)/pLysS cells with pOZ169 (GST-SpoVID$_{FL}$) in which the entire *spoVID* coding sequence was translationally fused to the *gst* gene (33). We used pOZ169 and primer pairs *spoVID*STOP1498D/*spoVID*-STOP1498R, *spoVID*-STOP1198D/*spoVID*-STOP1198R, *spoVID*STOP907D/*spoVID*-STOP907R, and *spoVID*-STOP607D/*spoVID*-STOP607R to replace codons 500, 400, 303, and 203 in *spoVID* with nonsense codons by using the QuickChange site-directed mutagenesis system (Stratagene) to obtain plasmids pTC52 (GST-SpoVID$_{499}$), pTC51 (GST-SpoVID$_{399}$), pTC50 (GST-SpoVID$_{302}$), and pTC49 (GST-SpoVID$_{202}$), respectively. Plasmids pTC52, pTC51, pTC50, and pTC49 were used to transform *E. coli* CC118(DE3)/pLysS, yielding strains AH2691, AH2690, AH2689, and AH2688, respectively (Table 1). Fusion of GST to residues 201 to 575 and 201 to 399 of SpoVID was done as follows. We PCR amplified DNA fragments of *spoVID* (codons 201 to 575 and 201 to 399) with primers *spoVID*+800D and *spoVID*1935R and the pOZ169 and pTC51 templates, respectively. The products were digested with BamHI and XhoI and cloned between the same sites of pOZ169, creating pTC61 (GST-SpoVID$_{201\text{–}575}$) and pTC62 (GST-SpoVID$_{201\text{–}399}$), which were then introduced into CC118(DE3)/pLysS, yielding AH2718 and AH2719, respectively (Table 1). In order to obtain strain AH2687, producing native GST (Table 1), we excised the *spoVID* coding region from pOZ169 (33) by digestion with BamHI and XhoI and filled-in the ends before autoligation. The resulting plasmid, pTC55, was used to transform CC118(DE3)/pLysS, creating AH2687 (Table 1).

Mutations in regions A and B of SafA. A PCR fragment comprising the entire *safA* coding region and 595 bp upstream of its start codon, generated with primers *safA*-595D and *safA*+1176R, was introduced in pCR2.1TOPO (Invitrogen) to create pTC75. Primers *safA*791D and *safA*834R were used to delete codons 203 to 206 (the PYYH motif) of *safA* in pTC75 by the QuickChange method, yielding pTC78. A chloramphenicol resistance (Cm^r) cassette was released from pMS38 (43) with XbaI and XhoI and inserted between the same sites of pTC78, generating pTC90. A PCR fragment encompassing codons 1 to 162 of *safA*, including 595 bp upstream of the *safA* start codon, was amplified with primers *safA*-595D and *safA*693R and inserted into pCR2.1TOPO (Invitrogene) to obtain pTC93 (SafA$_{N1\text{–}162}$). pTC93 was then digested with XbaI and XhoI, and a Cm^r cassette released from pMS38 (43) with the same enzymes was inserted to form pTC95. To fuse the *safA* promoter directly to codons 164 to 387, codons 1 to 163 were eliminated by amplification of pTC88 (obtained by cloning of the Cm^r cassette from pMS38 between the XbaI and XhoI sites of pTC75) with primers *safA*203R and *safA*677D, digestion of the resulting product with HincII, and religation to form pTC97 (SafA$_{C164\text{–}387}$). To delete residues 51 to 63 of SafA, a product generated from pTC88 with primers *safA*50-64D and *safA*50-64R was cut with SacII and religated, to yield pTC170 (SafA$_{\Delta G51\text{-}S63}$). pTC198 (SafA$_{\Delta G51\text{-}E57}$) and pTC199 (SafA$_{\Delta P58\text{-}S63}$) were constructed by cloning 143- and 146-bp fragments released from pTC196 and pTC197 (see above) with BbvII and EspI, respectively, between the same sites of pTC88 (see above). Alanine substitutions in SafA ($R_{55}A$, $K_{56}A$, $K_{59}A$, and $K_{62}A$) were obtained by the QuickChange method (Stratagene) by using pTC75 and primers *safA*Alamut50-64D and *safA*Alamut50-64R. The result was pTC172 (SafA$_{4\times Ala}$), from which pTC173 was made by introducing a Cm^r cassette (see above) between its XbaI and XhoI sites. All PCR products were sequenced. pTC90, pTC95, pTC97, pTC170, pTC190, pTC191, and pTC173 were transformed into *B. subtilis* AOB68 to form AH2781, AH2787, AH2788, AH4006, AH4090, AH4091, and AH4007, respectively (Table 1).

Green fluorescent protein (GFP) fusions. pTC204 (SafA$^+$-GFP) and pTC205 (SafA$_{\Delta G51\text{-}S63}$-GFP) were constructed as follows. First, the *safA* 3′ coding region (684 bp) was PCR amplified with primers *safA*677D and *safA-gfp*R. Second, a 714-bp fragment comprising the coding region of the *gfp* gene was PCR amplified with pEA18 (a gift from Alan Grossman) and primers *gfp*-30D and *gfp*mut2/749R. The resulting fragments were mixed and subjected to PCR with primers *safA*677D and *gfp*mut2/749R. The resulting 1,398-bp *′safA-gfp* fragment was cleaved with SmaI and EcoRI, and the 1,110-bp fragment was gel purified. DNA fragments corresponding to the 5′ regions of *safA*$^+$ or *safA*$_{\Delta G51\text{-}S63}$ were obtained by digestion of pTC75 and pTC170 (see above), respectively, with SmaI and NotI. The *safA*$^+$ and *safA*$_{\Delta G51\text{-}S63}$ fragments were cloned together with the *′safA-gfp* fragment between the NotI and EcoRI sites of pBEST501 (19) to yield pTC204 and pTC205, respectively. All PCR products were verified by sequencing. Strains AH4102 and AH4103 resulted from the integration of pTC204 or pTC205, respectively, at the *safA* locus of AOB68 via a single reciprocal (Campbell-type) crossover (Table 1). The *spoVID* null mutant AH1910 was transformed with chromosomal DNA of strains AH4102 and AH4103 to yield AH4107 and AH4108, respectively (Table 1).

Pull-down assays. In vitro pull-down assays were performed as described previously (33), except that 60 μl of a 50% slurry of glutathione-Sepharose beads (Amersham Biosciences) were used and the interaction mixtures were resuspended in a final volume of 30 μl of loading buffer, before analysis by sodium dodecyl sulfate (SDS)–12.5% polyacrylamide gel electrophoresis (PAGE) and immunoblotting.

Purification of spores and analysis of the spore coat. Spores were harvested by centrifugation of DSM cultures 24 h after the onset of sporulation, washed, and purified on step gradients of 20% to 50% Gastrografin (Schering) (8, 42). Coat proteins were extracted from purified spores at an optical density at 580 nm (OD_{580}) of about 2 and resolved by SDS–15% PAGE (14, 15). The gels were stained with Coomassie brilliant blue R-250 or transferred to nitrocellulose for immunoblot analysis as described below.

Western blot analysis. Pull-down samples and coat protein extracts were resolved by SDS-PAGE (12.5 and 15% gels, respectively) and immunoblot analysis conducted as previously described (8). Anti-SafA (32), anti-CotE (our unpublished work), and anti-CotG (43) antibodies were used at dilutions of 1:15,000, 1:1,000, and 1:7,500, respectively, whereas a horseradish peroxidase-conjugated secondary antibody (Sigma) was used at a dilution of 1:6,000. The immunoblots were developed with chemiluminescence reagents (Amersham Biosciences).

Microscopy. Samples (0.6 ml) of DSM cultures were collected about 2.5 and 4 h after the initiation of sporulation, resuspended in 0.2 ml of phosphate-buffered saline supplemented with 2 μl of a 1-mg ml^{-1} solution of 4,6-diamidino-2-phenylindole dihydrochloride (DAPI) for visualization of DNA. Microscopy was carried out as described previously (8, 36). DAPI staining allowed the identification of the prespore region and the ability to distinguish between cells that had just completed asymmetric division (with highly condensed prespore chromosomes) and those that had completed the engulfment process (diffuse DAPI signal in the prespore) (8, 36).

SPR experiments. Surface plasmon resonance (SPR) experiments were conducted on a BIACORE 2000 instrument with a CM5 sensor chip (Biacore International AB). For all measurements and immobilization procedures, the temperature was set to 25°C. The running buffer was HEPES-buffered saline (150 mM NaCl, 10 mM HEPES [pH 7.2], 3 mM EDTA, and 0.005% surfactant P20). Two flow cells (Fc) of the CM5 chip were prepared for the immobilization of GST (Fc3) and GST-SpoVID$_{202}$ (Fc4) by the standard amine coupling method provided by the manufacturer. Ligand immobilization was done at a flow rate of 10 μl/min with a buffer containing 10 mM sodium acetate, pH 3.9. The immobilization levels were established from 0.1 to 0.23 pmol/mm^2 (about 3,000 to 13,500 resonance units [RUs]). Two peptides were used as analytes: SafA-regionA (GVPVRKEPKAGKS) and SafA-Ala (GVPVAAEPAAGAS) (GenScript Corporation). Binding assays were performed in triplicate in HEPES-buffered saline with a 0.8 mM concentration of each analyte and a flow rate of 10 μl/min. The flow cells were regenerated with 10 mM glycine (pH 2.0) after each cycle. Injection times were 3 min for binding and 30 s for regeneration.

Protein identification by peptide mass fingerprinting. Proteins were excised from Coomassie brilliant blue R-250-stained gels and sent to the Microchemical Facility at Emory University for matrix-assisted laser desorption ionization–time-of-flight analysis.

RESULTS

The PYYH motif is involved in formation of the SafA-SpoVID complex. The PYYH motif, found in a phage display screen for peptides able to interact with SpoVID, is present in the C-terminal half of the SafA protein (residues 203 to 206)

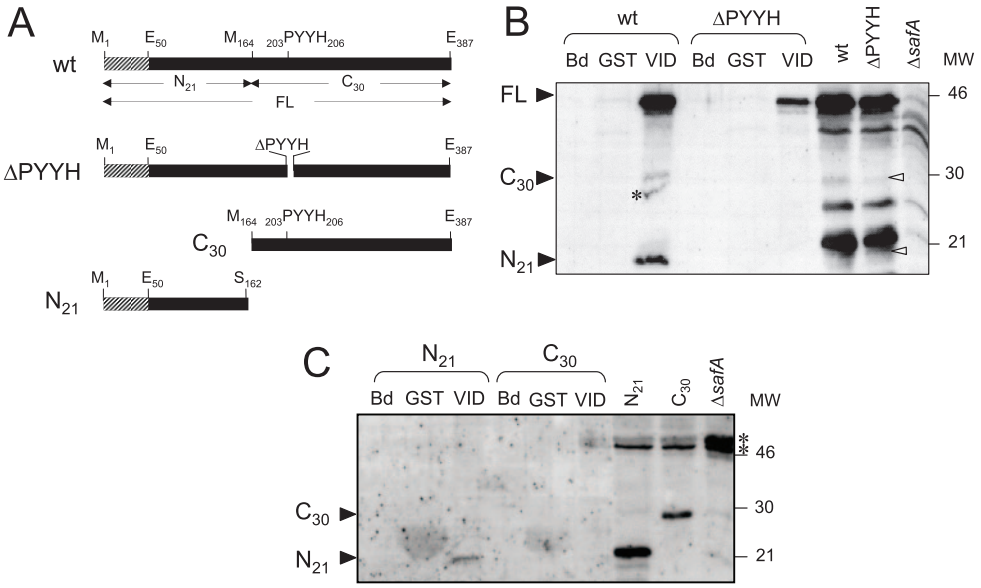

FIG. 1. Interaction of the N terminus of SafA with GST-SpoVID. (A) The 387-residue-long wild-type (wt) SafA protein and SafA variants deleted for residues 203 to 206 (ΔPYYH), for the N-terminal first 163 residues ($C_{164–387}$, corresponding to the $SafA_{C30}$ form), or missing the last C-terminal 225 residues ($N_{1–162}$, corresponding to the $SafA_{N21}$ form). The striped pattern represents the LysM domain (first 50 residues) of SafA. Other relevant residues are also indicated. SafA accumulates in sporulating cells in three main forms: $SafA_{FL}$ (45 kDa), a C-terminal form ($SafA_{C30}$, 30 kDa), and an N-terminal form ($SafA_{N21}$, 21 kDa). (B and C) Interaction of immobilized GST-SpoVID with wild-type SafA and $SafA_{\Delta PYYH}$ (B) and with the $SafA_{C30}$ and $SafA_{N21}$ forms (C) present in extracts at hour 4 of sporulation. The extracts were incubated with GST-SpoVID (VID for simplicity), with GST bound to glutathione-Sepharose beads, or with the beads alone (Bd). Pulled-down proteins were resolved by SDS-PAGE and immunoblotted with an anti-SafA antibody. The positions of $SafA_{FL}$, $SafA_{C30}$, and $SafA_{N21}$ (black arrowheads), of cross-reactive species (asterisks), and of molecular mass markers (in kilodaltons) are indicated. The last three lanes in panel C show the immunoblot analysis of the extracts from strains producing $SafA_{N21}$ or $SafA_{C30}$, used in the pull-down assays, and of a Δ*safA* mutant, with the anti-SafA antibody.

(Fig. 1A) (32). To investigate whether the PYYH motif is involved in the interaction of SafA with SpoVID, we constructed a mutant expressing a form of SafA lacking residues 203 through 206, or $SafA_{\Delta PYYH}$ (Fig. 1A). Then, we tested whether a GST-SpoVID purified protein was able to pull down $SafA_{\Delta PYYH}$. GST-SpoVID and GST alone were overproduced in *E. coli*, bound to glutathione-Sepharose beads, and incubated with extracts from wild-type *B. subtilis* or the *safA*$_{\Delta PYYH}$ mutant prepared at hour 4 of sporulation. We also incubated the extracts with beads alone as a control. After extensive washing, retained proteins were resolved by SDS-PAGE, blotted, and probed with an anti-SafA antibody (see Materials and Methods). The three main forms of SafA that accumulate in sporulating cells, $SafA_{FL}$ (45 kDa), C-terminal ($SafA_{C30}$, 30 kDa), and N-terminal ($SafA_{N21}$, 21 kDa), were pulled down by the glutathione-Sepharose beads to which GST-SpoVID had been bound but not by beads containing GST or by the beads alone (Fig. 1B). Similar experiments showed that the full-length form of SafA deleted for the PYYH motif ($SafA_{\Delta PYYH}$) was also retained by GST-SpoVID but not by GST or the beads (Fig. 1B). In contrast, the $SafA_{C30}$ and $SafA_{N21}$ forms in the $SafA_{\Delta PYYH}$ strain were not retained by the GST-SpoVID beads (Fig. 1B). Yeast two-hybrid experiments have shown that $SafA_{N21}$ can directly interact with SpoVID, but the interaction seemed weaker than the interaction of $SafA_{N21}$ with $SafA_{FL}$ (32; also see below). $SafA_{N21}$ may not bind directly to SpoVID in the pull-down assay because it is out-competed by $SafA_{FL}$ or by $SafA_{\Delta PYYH}$. This suggests that $SafA_{N21}$ is recruited by the SpoVID-SafA complex but not by the SpoVID-$SafA_{\Delta PYYH}$ complex (Fig. 1B). This also suggests that a site able to interact with SpoVID is likely to exist in the N-terminal region of SafA (also see below). In the yeast two-hybrid analysis of Ozin et al. (32), no interaction was detected between $SafA_{C30}$ and SpoVID, and GST-$SafA_{C30}$ was able to pull down only itself from extracts of sporulating cells (33). Thus, it appears that the $SafA_{C30}$ form interacts with the SpoVID-SafA complex but not with the SpoVID-$SafA_{\Delta PYYH}$ complex (Fig. 1B). Together, the results suggest that the PYYH motif in SafA (hereafter named region B) is not essential for the interaction of full-length SafA with SpoVID but appears to affect the SpoVID-SafA complex in a way that interferes with its capacity to recruit the $SafA_{N21}$ and $SafA_{C30}$ forms of SafA.

Residues 51 to 63 of SafA are essential for its interaction with SpoVID in vitro. The results in preceding section, together with previous results showing that $SafA_{N21}$ interacts with SpoVID in a yeast two-hybrid assay (32), strongly suggest that a second site in SafA (presumably in its N-terminal region) must exist that promotes its interaction with SpoVID. To test this, we performed pull-down assays using *B. subtilis* mutants producing only the $SafA_{N21}$ (residues 1 to 162) or $SafA_{C30}$ (residues 164 to 387) forms (Fig. 1A). The results in Fig. 1C show that only $SafA_{N21}$ (first 162 residues) was retained by GST-SpoVID, indicating that this region contains residues sufficient for the interaction with SpoVID. The observation that, when produced alone, "wild-type" $SafA_{C30}$ (i.e., carrying region B) was not retained by GST-SpoVID (Fig. 1C)

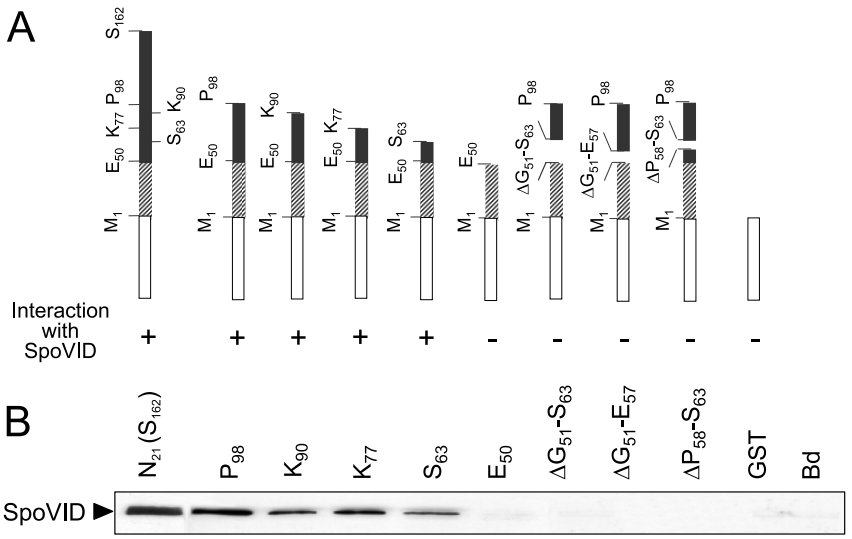

FIG. 2. Deletion mapping of region A in SafA. (A) The various GST-SafA fusions used, with the white box representing GST (not to scale) and the striped pattern (residues 1 to 50) the LysM motif. The plus or minus symbol below each diagram indicates an interacting or noninteracting fusion protein, respectively. (B) Results of pull-down assays using truncated forms of GST-SafA and SpoVID. A cell extract prepared from an *E. coli* strain overproducing native SpoVID was incubated with the various purified GST-SafA truncated forms containing the following residues, as indicated: 1 to 162 (S_{162}), 1 to 98 (P_{98}), 1 to 90 (K_{90}), 1 to 77 (K_{77}), 1 to 63 (S_{63}), 1 to 50 (E_{50}), 1 to 98 but excluding residues 51 to 63 (ΔG_{51}-S_{63}), 1 to 98 but excluding residues 51 to 57 (ΔG_{51}-E_{57}), and 1 to 98 but excluding residues 51 to 63 (ΔP_{58}-S_{63}). The same extracts were incubated with GST bound to glutathione-Sepharose beads or with beads alone (Bd), as controls. Pulled-down proteins were resolved by SDS-PAGE and immunoblotted with an anti-SpoVID antibody (see Materials and Methods). The position of SpoVID is indicated by the black arrowhead.

is consistent with results of previous studies in which $SafA_{C30}$ and SpoVID did not interact (32, 33).

To determine whether a specific region within the first 162 residues of SafA was involved in the interaction with SpoVID, we overproduced several truncated forms of SafA as GST fusion proteins in *E. coli*. The forms of SafA produced contained residues 1 to 162 (herein designated S_{162}, the letter and number referring to the identity and position of the last residue in the SafA fragment), 1 to 98 (P_{98}), 1 to 90 (K_{90}), 1 to 77 (K_{77}), 1 to 63 (S_{63}), or 1 to 50 (E_{50}) (Fig. 2A). All of the truncated forms of SafA were able to pull down untagged SpoVID overproduced in *E. coli* except the form containing just the first 50 residues of SafA (E_{50}), which correspond to its LysM domain (Fig. 2B). The results indicate that the region of 13 amino acids from residues 51 to 63 in SafA (GVPVRKEP KAGKS, hereafter referred to as region A), just downstream of the LysM domain, is sufficient for the interaction with SpoVID in vitro. In confirmation of this assumption, deletion of residues 51 to 63 (ΔG_{51}-S_{63}) from the P_{98} form prevented its interaction with SpoVID (Fig. 2A and B). In an attempt to define region A further, residues 51 to 57 (ΔG_{51}-E_{57}, i.e., the N-terminal half of region A) or 58 to 63 (ΔP_{58}-S_{63}, its C-terminal half) were removed from the P_{98} form (Fig. 2A). Neither of the new versions of P_{98} was able to pull down SpoVID (Fig. 2B), indicating that residues on both halves of region A are required for the interaction with SpoVID in vitro.

Region A of SafA directly contacts SpoVID. All three deletion forms of SafA ($SafA_{\Delta G51\text{-}S63}$, $SafA_{\Delta G51\text{-}E57}$, and $SafA_{\Delta P58\text{-}S63}$) accumulated to wild-type levels in extracts from *B. subtilis* cells harvested at hour 4 of sporulation (Fig. 3B) but failed to bind to immobilized GST-SpoVID (not shown). Therefore, the complete or partial deletion of region A does not alter the stability of SafA significantly. (Note that for reasons we do not presently understand, the accumulation of the $SafA_{N21}$ and $SafA_{C30}$ forms varied among the three *safA* deletion mutants and in comparison to the wild type, as shown in Fig. 3B; however, we also note that only $SafA_{FL}$ is required for the formation of lysozyme-resistant spores [33].) We also tested the effect of alanine substitutions within region A on the interaction with SpoVID. The results shown in Fig. 3B indicate that the replacement of residues R_{55}, K_{56}, K_{59}, and K_{62} in region A by alanines ($R_{55}A$, $K_{56}A$, $K_{59}A$, and $K_{62}A$), to produce the $SafA_{4\times Ala}$ form (Fig. 3A), did not interfere with the accumulation of SafA in extracts of sporulating cells. However, $SafA_{4\times Ala}$ was not pulled down by GST-SpoVID in vitro (Fig. 3C), suggesting that residues R_{55}, K_{56}, K_{59}, and K_{62} in SafA are directly involved in the interaction with SpoVID.

To independently test whether region A of SafA is directly involved in the interaction with SpoVID, we conducted SPR experiments with immobilized GST or GST-$SpoVID_{202}$ (a truncated form of SpoVID that binds SafA in pull-down assays as well as the wild-type protein; see below) and peptides corresponding to either region A (SafA-regionA, GVPVRKEPK AGKS) or to region A bearing the four alanine substitutions (SafA-Ala, GVPVAAEPAAGAS). GST and GST-$SpoVID_{202}$ were immobilized in flow cells 3 and 4 of a CM5 sensor chip, respectively (see Materials and Methods), and the SafA-regionA or SafA-Ala peptides were tested for binding with a BIAcore system (see Materials and Methods). We obtained 27.7 ± 4.0 RUs as the response for binding of SafA-regionA to GST-$SpoVID_{202}$ (in flow cell 4) but only -0.7 ± 0.4 RUs for binding of the SafA-Ala peptide (note that the negative values are caused by differences in the refractive indices between the buffer with or without the ligand). No binding was detected for

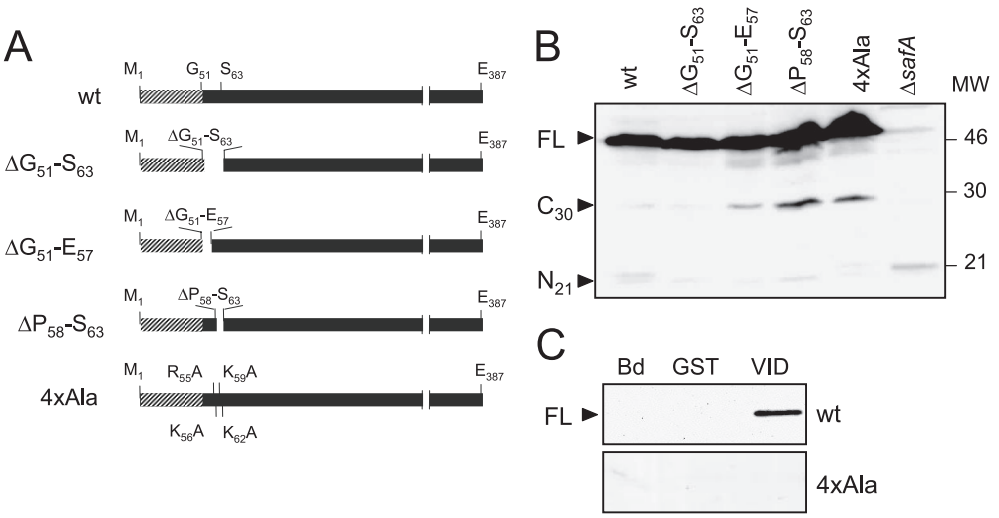

FIG. 3. Accumulation of SafA variants in sporulating *B. subtilis* and analysis of their interaction with GST-SpoVID. (A) The 387-amino-acid wild-type (wt) SafA protein and SafA variants deleted for residues 51 to 63 (ΔG_{51}-S_{63}), 51 to 57 (ΔG_{51}-E_{57}), and 58 to 63 (ΔP_{58}-S_{63}) or with alanine substitutions of residues R_{55}, K_{56}, F_{62}, and K_{59} (4×Ala). The LysM domain (residues 1 to 50) in SafA is indicated by the striped pattern. (B) Accumulation of SafA variants in cell extracts prepared from cultures of *B. subtilis* at hour 4 of sporulation. The proteins were resolved by SDS-PAGE and immunoblotted with an anti-SafA antibody. The positions of the full-length (FL), $SafA_{C30}$, and $SafA_{N21}$ forms of SafA (black arrowheads), of a cross-reactive species (asterisk), and of molecular mass markers (in kilodaltons) are indicated. (C) Interaction of SafA (wild type) or the $SafA_{4\times Ala}$ variant present in extracts from sporulating *B. subtilis* with GST-SpoVID (VID). Cell extracts prepared from wild-type *B. subtilis* and from strains producing $SafA^+$ or $SafA_{4\times Ala}$ were incubated with GST-SpoVID or GST immobilized on glutathione-Sepharose beads or with the beads alone (Bd), and the pulled-down proteins were resolved by SDS-PAGE and immunoblotted with an anti-SafA antibody (see Materials and Methods). The position of $SafA_{FL}$ is indicated by the black arrowhead.

either the SafA-regionA or SafA-Ala peptide (0.9 ± 0.4 RUs and −1.7 ± 0.4 RUs, respectively) to immobilized GST alone (in flow cell 3). These results strengthen our inference that residues in region A of SafA are involved in the interaction with SpoVID.

The LysM motifs in both SpoVID and SafA are not involved in their interaction. The observation that $SafA_{N21}$ interacted with SpoVID in a yeast two-hybrid assay led Ozin and coworkers to propose that the two proteins could interact via their LysM domains (32). However, the results presented above indicate that SafA does not interact with SpoVID via its LysM domain (fusion E_{50} in Fig. 2). To examine whether the LysM domain present at the C terminus of SpoVID was involved in the interaction with SafA, we conducted pull-down assays using GST fusions to $SpoVID_{FL}$ or to SpoVID deleted in its last 76 residues (T_{499}), which encompass the LysM motif (Fig. 4A). The results shown in Fig. 4B indicate that both versions of SpoVID were able to pull down all main forms of SafA present in *B. subtilis* extracts, that is, $SafA_{FL}$, $SafA_{N21}$, and $SafA_{C30}$. These experiments suggest that the LysM domain of SpoVID is not involved in the interaction with SafA. To determine whether SafA binds to a specific section of the 575-residue-long SpoVID protein, additional pull-down assays were carried out with fusions of GST to truncated forms of SpoVID corresponding to residues 1 to 202 (R_{202}), 1 to 302 (A_{302}), and 1 to 399 (N_{399}) (Fig. 4A). We found that all of the truncated forms of SpoVID were able to pull down the main forms of SafA present in *B. subtilis* extracts (Fig. 4B). Hence, the first 202 residues of SpoVID are sufficient for the interaction with SafA. To determine whether this region is necessary for the interaction, we performed similar pull-down experiments using fusions of GST to truncated forms of SpoVID lacking either its first 200 residues (L_{201}-A_{575}) or comprising only residues 201 to 399 (L_{201}-N_{399}) (Fig. 4A). Neither of these fusion proteins retained SafA (Fig. 4B). We infer from these results that the LysM domain of SpoVID is not involved in the interaction with SafA. We further infer that the N-terminal 202 residues of SpoVID are necessary for the interaction with SafA (also see below).

Region A but not region B of SafA is required for proper coat assembly. Spores of a *safA* null mutant have abnormal coats, from which several coat components are missing, and are susceptible to lysozyme (32, 40). Because the $SafA_{\Delta G51\text{-}S63}$, $SafA_{\Delta G51\text{-}E57}$, $SafA_{\Delta P58\text{-}S63}$, and $SafA_{4\times Ala}$ mutant forms accumulated to normal levels in *B. subtilis* yet failed to interact with SpoVID, we wanted to assess the impact of mutations in region A in the assembly of the spore coat. Spores of the various region A mutants, along with wild-type and *safA* null mutant spores, were purified, and the collection of coat polypeptides was extracted and analyzed by SDS-PAGE (Fig. 5A). *safA* null mutant spores lack the 36-kDa CotG protein, as judged by Coomassie staining of gels of coat protein extracts (40) (Fig. 5A). A 36-kDa band, and to a lesser extent a band of about 32 kDa, seen in wild-type coat extracts appeared reduced from the extracts of the various *safA* mutants (Fig. 5A). These represent 36- and 32-kDa forms of CotG (43), as verified by immunoblot analysis (not shown). In agreement with the reduction in the representation of CotG, the 66-kDa form of CotB (as verified by immunoblot analysis; data not shown), whose formation depends on CotG (43), was also reduced in all *safA* mutants (Fig. 5A). Two other bands that appeared reduced in all of the *safA* mutants are labeled *a* and *b* in Fig. 5A. Mass spectrometry analysis indicated that these bands contained CotJC and YhcN (band *a* [38]) and CotC sequences

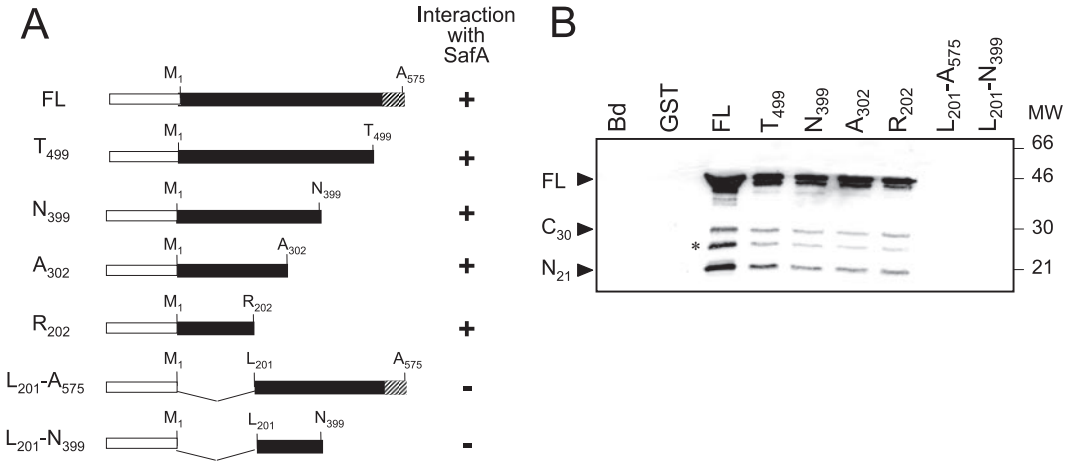

FIG. 4. SafA interacts with a defined region of SpoVID. (A) Schematic representation of fusions of the 575-residue-long $SpoVID_{FL}$ protein (FL), as well as forms of SpoVID containing residues 1 to 499 (T_{499}), 1 to 399 (N_{399}), 1 to 302 (A_{302}), 1 to 202 (R_{201}), 201 to 575 (L_{201}-A_{575}), and 201 to 399 (L_{201}- N_{399}), to GST. The white box represents GST (not to scale), and the LysM motif (residues 525 to 575) corresponds to the striped pattern. The plus or minus symbol on the right side of each diagram indicates a protein interacting or not interacting with SafA, respectively. (B) Results of pull-down assays performed with the various purified truncated forms of SpoVID fused to GST and extracts from wild-type *B. subtilis* AOB90 (Table 1) prepared at hour 4 of sporulation. The immunoblot was probed with an anti-SafA antibody. The same extracts were also incubated with immobilized GST or with glutathione beads alone (Bd). The black arrowheads indicate the positions of the full-length, $SafA_{C30}$, and $SafA_{N21}$ forms of SafA, and the asterisk indicates a degradation product of SafA. Molecular mass markers (in kilodaltons) are also indicated.

(band *b* [10]). In contrast, band *c* appeared more abundant in the extracts from $SafA_{\Delta G51\text{-}S63}$ spores than from the wild type (Fig. 5A), whereas band *d* was more abundant in the extracts from $SafA_{\Delta G51\text{-}E57}$ spores (Fig. 5A). We found band *c* to contain GerQ and band *d* to contain SodA, previously found in association with the spore coat and involved in the oligomerization of CotG (17, 25). The differences between the various SafA deletion mutants may reflect subtle differences in the capacity of residues in the N- and C-terminal halves of region A to promote the interaction of SafA with SpoVID (also see below). In contrast, deletion of region B did not affect in a discernible way the profile of Coomassie-stained coat polypeptides (data not shown). Together, the results show alterations of the coat structure caused by lesions in region A of SafA that are largely coincident with those caused by a *safA* null allele. We infer that the coat structural deficiencies seen in region A mutants are caused by the impaired interaction of SafA with SpoVID.

Region A in SafA is required for the formation of a functional coat. Spores of a *safA* null mutant are susceptible to lysozyme (32, 40). To examine whether the mutations in region A and the associated perturbations at the level of the coat polypeptide composition were sufficient to affect this functional property of the coat, spores of the various region A mutants were assayed for lysozyme resistance. The results in Table 2 show that spores produced by mutants lacking residues

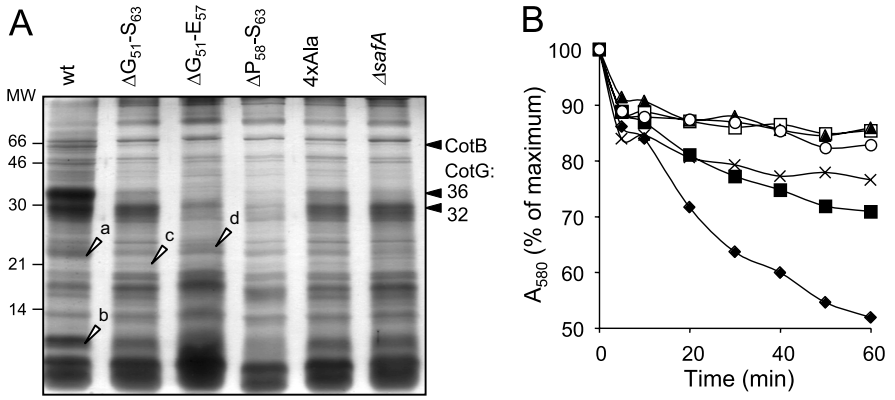

FIG. 5. Spores of region A mutants have an altered coat and impaired germination. (A) Coomassie-stained gel of SDS-PAGE-resolved coat protein extracts prepared from purified spores of the wild type (wt) (lane 1) and the $SafA_{\Delta G51\text{-}S63}$ (lane 2), $SafA_{\Delta G51\text{-}E57}$ (lane 3), $SafA_{\Delta P58\text{-}S63}$ (lane 4), $SafA_{4\times Ala}$ (lane 5), and Δ*safA* (lane 6) mutants. Open arrowheads point to bands (a to d) that were excised and subjected to mass spectrometry analysis (see Materials and Methods). The positions of bands corresponding to the 66-kDa form of CotB and to the 32- and 36-kDa forms of CotG are indicated by black arrowheads. (B) Germination responses to AGFK of purified spores of the wild type (closed diamonds) and the $SafA_{4\times Ala}$ (closed squares), $SafA_{\Delta G51\text{-}S63}$ (open squares), $SafA_{\Delta G51\text{-}E57}$ (closed triangles), $SafA_{\Delta P58\text{-}S63}$ (crosses), and Δ*safA* mutants (open circles). Germination was monitored by following the decrease in absorbance at 580 nm over time (in minutes) and is shown as the percentage of the OD_{580} at the beginning of the assay.

TABLE 2. Spore resistance properties

Strain	Relevant genotype	Cell count (CFU/ml)[a]		
		Viable	Heat resistant	Lysozyme resistant
MB24	Wild type	8.3×10^8	7.6×10^8	6.5×10^8
AOB68	Δ*safA*	5.0×10^8	6.1×10^8	3.1×10^7
AH2781	$safA_{\Delta PYYH}$	7.9×10^8	5.1×10^8	4.3×10^8
AH4006	$safA_{\Delta G51\text{-}S63}$	4.9×10^8	3.8×10^8	7.6×10^7
AH4007	$safA_{4\times Ala}$	4.4×10^8	4.7×10^8	2.2×10^8
AH4090	$safA_{\Delta G51\text{-}E57}$	2.3×10^8	2.3×10^8	2.7×10^7
AH4091	$safA_{\Delta P58\text{-}S63}$	4.1×10^8	3.4×10^8	7.0×10^7

[a] Total (viable) and heat- and lysozyme-resistant cell counts were determined as described in Materials and Methods.

51 to 63 (region A), 51 to 57, or 58 to 63 of SafA have a degree of susceptibility to lysozyme treatment in the range of that observed for spores of a *safA* null mutant (about 10^7 lysozyme-resistant spores/ml of culture, compared to 10^8 for wild-type spores). None of the mutations in region A affected spore heat resistance (Table 2), a property that relies on proper cortex formation, and hence the effects herein described are specifically related to the assembly of the spore coat. We have also found that spores of the $SafA_{\Delta PYYH}$ mutant are fully resistant to lysozyme (Table 2), an observation that is in agreement with absence of any discernible alteration in the profile of Coomassie-stained coat polypeptides (see above). This reinforces the suggestion that the PYYH motif is not a critical determinant for the SafA-SpoVID interaction (see above). Surprisingly however, spores of the $SafA_{4\times Ala}$ mutant were also found to be resistant to lysozyme (Table 2). Presumably, the alanine substitutions within region A still permit some degree of interaction of SafA with SpoVID in vivo, sufficient to support spore lysozyme resistance. In support of this interpretation, we found that when examined for their germination in response to a mixture of asparagine, glucose, fructose, and KCl (AGFK), a property that is dependent on *safA* (40), spores of the $SafA_{4\times Ala}$ mutant showed an intermediate phenotype between the wild type and the *safA* null mutant (Fig. 5B). In contrast, the results in Fig. 5B show that spores of the $SafA_{\Delta G51\text{-}E57}$ and $SafA_{\Delta G51\text{-}S63}$ mutants were as impaired in AGFK-induced germination as were spores of the *safA* null mutant. Spores of the $SafA_{\Delta P58\text{-}E63}$ mutant however, showed a response to AGFK that closely paralleled that of the $SafA_{4\times Ala}$ mutant (Fig. 5B), suggesting that residues in the N-terminal half of region A have a greater impact on the SafA-SpoVID interaction, at least as assessed by this spore property. Overall, the finding that mutations in region A led to a germination phenotype that largely mimics that of a *safA* null mutant strengthens the view that the function of SafA critically depends on its interaction with SpoVID.

Targeting of SafA to the surface of the developing spore depends on its interaction with SpoVID. Lastly, we examined the impact of eliminating region A on the subcellular localization of SafA in developing cells. SafA is targeted to the surface of the developing spore early in the process of coat assembly, just after formation of the asymmetric septum that partitions the sporulating cell into the mother cell and prespore compartments (33). Targeting of SafA occurs in two stages, as defined by immunofluorescence microscopy: first, SafA localizes as a spot at the mother cell/prespore border in a SpoVID-independent manner, and later SafA migrates around the developing spore in a SpoVID-dependent manner (33). Both wild-type SafA and $SafA_{\Delta G51\text{-}S63}$ were fused to GFP, and the localizations of both fusion proteins were studied by fluorescence microscopy (Fig. 6A). First, we established that spores of a strain expressing SafA-GFP were resistant to lysozyme, indicating that the fusion protein is largely functional (data not shown). Then, we studied the pattern of localization of both fusion proteins in the wild type and in a *spoVID* congenic mutant 2.5 and 4 h after the onset of sporulation. In wild-type cells, SafA-GFP was first targeted to the mother cell/prespore border as a spot (Fig. 6A, panel a) and later started migrating around the prespore to form a cap covering the spore end distal to the cell pole (Fig. 6A, panel e) in a *spoVID*-dependent mode (Fig. 6A, panel f). In the wild type, the "spot" pattern was associated with cells that had just undergone asymmetric division but had not initiated engulfment, whereas the "cap" pattern was found for cells that had initiated engulfment (the morphological stages were scored by DAPI staining, as described in Materials and Methods). The quantification of these results is shown in Fig. 6B. Note that the "spot" pattern pre-

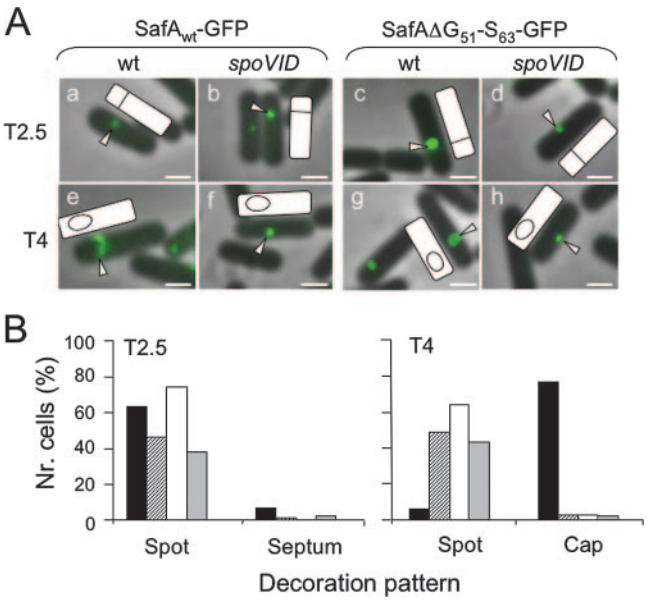

FIG. 6. Region A is important for the SpoVID-dependent localization of SafA. (A) Cells expressing a functional fusion of SafA to GFP (SafA-GFP) or $SafA_{\Delta G51\text{-}S63}$-GFP in the wild type (wt) (panels a, c, e, and g) or in a *spoVID* background (panels b, d, f, and h) were observed by fluorescence microscopy at 2.5 h (panels a to d) and 4 h (panels e to h) after the onset of sporulation in DSM. Overlay images of GFP fluorescence and phase-contrast microscopy are shown in all panels. White arrowheads point to the region showing fluorescence in a selected cell, and the position of the prespore (as determined by DAPI chromosomal staining; not shown) is shown in the schematic representation of the same cell included in each panel. The scale bar represents 1 μm. (B) Quantification of GFP decoration patterns. A minimum of 75 cells were scored for fluorescence patterns designed by spot, septum, or cap at hours 2.5 and 4 in cultures of both the wild type and *spoVID* mutant expressing either SafA-GFP or $SafA_{\Delta G51\text{-}S63}$-GFP: AH4102 (SafA-GFP; black bars), AH4103 ($SafA_{\Delta G51\text{-}S63}$-GFP; striped bars), AH4107 (SafA-GFP *spoVID*; white bars), and AH4108 ($SafA_{\Delta G51\text{-}S63}$-GFP *spoVID*; gray bars).

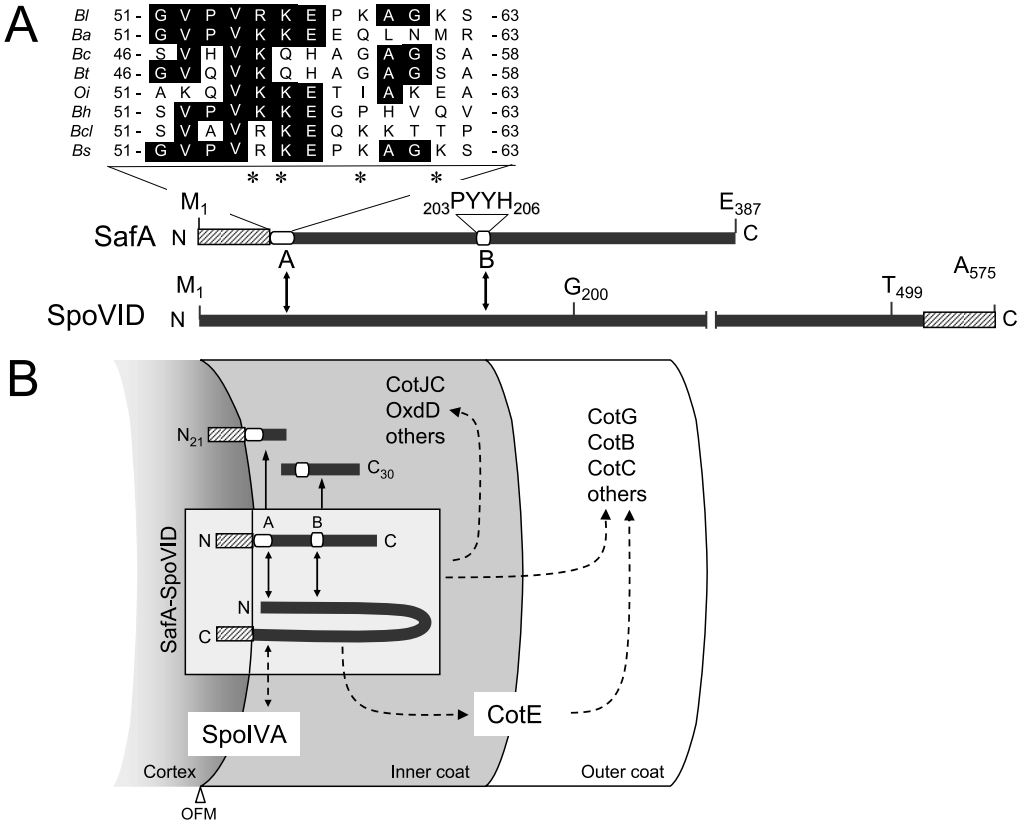

FIG. 7. Interaction of SafA with SpoVID and role of the complex in spore coat assembly. (A) Structure of SafA and SpoVID, with the LysM motifs (striped pattern) shown in each protein, as well as regions A (residues 51 to 63) and B (PYYH motif) in SafA (white boxes). Also shown is an alignment of the sequence of region A with the following SafA orthologs: *Bs*, *B. subtilis* 168 (accession number NP_390662); *Bl*, *B. licheniformis* ATCC14580 (YP_080055); *Bt*, *B. thuringiensis* serovar konkukian strain 97-27 (YP-038478); *Ba*, *B. anthracis* "Ames ancestor" (YP_021306); *Bc*, *B. cereus* ATCC 10987 (NP_980805); *Bcl*, *B. clausii* KSM-K16 (YP_175046); *Bh*, *B. halodurans* C-125 (NP_242087); Oi, *Oceanobacillus iheyensis* HTE831 (NP_692961). Identical residues are highlighted, and asterisks indicate the alanine substitutions in $SafA_{4\times Ala}$. (B) Model for the localization of SafA and SpoVID. Both SafA and SpoVID localize at the cortex/coat interface, delimited by the outer forespore membrane (OFM). Targeting of SpoVID to this region requires SpoIVA and may involve a direct interaction between the two proteins. SafA is initially targeted to the cortex/coat interface independently of SpoVID, a step that may involve its LysM domain. In a second stage, SafA interacts with SpoVID via regions A and B to form the SpoVID-SafA complex (shown within a box), which allows SafA to encircle the spore. SafA or the SpoVID-SafA complex controls the assembly of a subset of inner and outer coat proteins (i.e., CotE controlled), and SpoVID is essential for maintaining the coat anchored to the cortex, in part because of its requirement for keeping CotE at the inner coat/outer coat interface. Solid arrows indicate a direct interaction, whereas broken arrows indicate direct or indirect interactions.

dominated in samples at hour 2.5 of sporulation and was not affected by mutation of *spoVID*, whereas accumulation of the "cap" pattern, which predominated at hour 4, required expression of *spoVID* (Fig. 6B). These results agree with those of Ozin and coworkers (33), except that in their experiments SafA was found as caps covering both spore ends. However, the signal at the pole-proximal spore end was always weaker than the signal at the spore end away from the cell pole (33). We emphasize that our SafA-GFP fusion is functional, and we presume that the fluorescence at the pole-proximal spore end is not detected under our conditions. In any event, a strikingly different pattern was found for the $SafA_{\Delta G51\text{-}S63}$-GFP fusion protein. $SafA_{\Delta G51\text{-}S63}$-GFP was still targeted at an early time (hour 2.5) to the asymmetric septum, where it accumulated as a spot (Fig. 6A, panels c and d). However, for this protein the incidence of the "spot" pattern persisted at hour 4, at the expense of the "cap" pattern, whose representation was severely curtailed regardless of the presence of a functional *spoVID* locus (Fig. 6A, panels g and h, and Fig. 6B). We conclude that deletion of region A in SafA strongly interferes with the SpoVID-dependent stage of SafA localization, and we infer that the interaction of SafA with SpoVID via region A is required for the correct localization of SafA to the developing coat.

DISCUSSION

Previous work has suggested that the PYYH motif (region B) in the C-terminal half of SafA, found in a phage display screen for peptides able to interact with SpoVID, could mediate the interaction of SafA with SpoVID in vivo (32, 33) (Fig. 7A). However, a second region of interaction was postulated to exist in the N-terminal half of SafA (33). We now show that such a region indeed exists in the N-terminal half of SafA (Fig. 7A). $SafA_{N21}$ (but not $SafA_{C30}$) could be pulled out by immobilized GST-SpoVID, and deletion mapping indicated that a region of 13 amino acids encompassing residues 51 to 63 of SafA, or region A, is sufficient for the interaction with SpoVID

in vitro (Fig. 2). Moreover, region A is required for the interaction with SpoVID and for the proper subcellular localization and function of SafA in vivo (Fig. 5 and 6). Importantly, variants of SafA with the complete or partial deletion of region A accumulated in *B. subtilis* but failed to promote proper assembly of the coat, lysozyme resistance, and normal spore germination, mimicking the phenotypes of a *safA* null mutant (32, 40). That region A of SafA is directly involved in the interaction with SpoVID is supported by two lines of evidence. First, a form of SafA with alanine substitutions in region A accumulated in vivo but could not be pulled down by GST-SpoVID. Second, a peptide consisting of the wild-type region A sequence, but not a related peptide bearing the same four alanine substitutions (above), was able to bind to immobilized GST-SpoVID.

Region B is also involved in SpoVID-SafA complex formation (33) (Fig. 7A), as its deletion did not allow immobilized SpoVID to pull down $SafA_{N21}$ or $SafA_{C30}$ (Fig. 1B). This suggests that $SafA_{N21}$ and $SafA_{C30}$ are not bound directly by SpoVID but rather are recruited by the complex formed by SafA and SpoVID. $SafA_{N21}$ binds to SpoVID when made alone but may be outcompeted by $SafA_{FL}$ or by $SafA_{\Delta PYYH}$, in agreement with the yeast two-hybrid analysis of Ozin and coauthors, which suggested a $SafA_{N21}$-SpoVID interaction weaker than that of $SafA_{N21}$ with $SafA_{FL}$ (33). $SafA_{C30}$, in turn, was not pulled down by GST-SpoVID when made alone (Fig. 1C), also in agreement with an earlier study which found that GST-$SafA_{C30}$ could not bind to SpoVID in the absence of $SafA_{FL}$ and that no interaction was detected between $SafA_{C30}$ and SpoVID in a yeast two-hybrid assay (33). In any case, while deletion of region A causes spore susceptibility to lysozyme, deletion of region B does not (Table 2; also see below). Taken together, the results suggest that region A is essential for the interaction of SafA with SpoVID and that region B (while not essential) favors the interaction and/or allows the SafA-SpoVID complex to attain the correct topology for binding of $SafA_{N21}$ and $SafA_{C30}$ (Fig. 7B).

The consequences of lesions in region A were reminiscent of the effects of a *safA* null allele. First, spores of the various mutants had aberrant coats, from which CotG (both the 32- and 36-kDa forms), CotB, CotC, and possibly CotJC (10, 15, 37, 38) were reduced or missing (Fig. 5A). Second, as did those of a *safA* null mutant (40), spores of all region A mutants showed impaired germination in response to AGFK (Fig. 5B). Lastly, with the exception of the $SafA_{4\times Ala}$ mutant, the partial or complete deletion of region A results in spores that were, like those of the *safA* null mutant (32, 40), susceptible to lysozyme (Table 2). We take these results as indicating that the interaction of SafA (via region A) with SpoVID is responsible for its morphogenetic function in coat assembly. The differences in the composition of the coat extracts, as well as in the germination responses among the various mutants and the lysozyme resistance of the $SafA_{4\times Ala}$ mutant, suggest that the various mutations affect the interaction in vivo to various degrees, influencing the assembly of other downstream components.

SafA localizes to the developing spore in two stages (33). First it localizes as a dot at the mother cell/prespore border in a SpoVID-independent manner. Second, under the guidance of SpoVID, it encircles the prespore. Our results indicate that while a functional fusion of SafA to GFP undergoes assembly following the two-stage pathway described for the native protein, a SafA-GFP fusion lacking region A did not initiate the SpoVID-dependent stage (Fig. 6). These results suggest that SafA interacts with SpoVID via region A after the initial targeting of both proteins to the nascent coat and that this interaction allows SafA to follow SpoVID in its movement around the prespore as engulfment proceeds. We suggest that SpoVID directly interacts with a factor localized close to or at the prespore outer membrane that itself is pulled around the prespore during engulfment. This factor could be the morphogenetic protein SpoIVA, which localizes close to the prespore outer membrane and upon which the localization of SpoVID is dependent (12, 33) (Fig. 7B).

We do not yet know how is SafA initially targeted to the surface of the developing spore. It is possible that the initial (SpoVID-independent) targeting of SafA, which then permits the interaction with SpoVID, involves its LysM domain. For example, the tandem LysM domains of another coat protein component, YaaH, are sufficient to direct β-lactamase to the surface of the developing spore (23, 24). However, we could not yet test for the involvement of the LysM domain in the initial targeting of SafA because deletion of this region results in an unstable protein that does not accumulate in sporulating cells (our unpublished results).

Formation of the SafA-SpoVID complex involves defined regions in SafA (regions A and B) and SpoVID (first 202 residues), suggesting that SafA and SpoVID have a modular design. Other morphogenetic proteins, for example, SpoIVA and CotE, also appear to have a modular design, with regions specifically involved in their targeting, multimerization, and interactions with additional coat components (3, 7, 21, 28, 34). Both SafA and SpoVID localize to the cortex/coat interface, where they promote attachment of the coat to the cortex (4, 12, 32, 40; also this work), and both proteins and their complex are likely to interact with additional coat components (6, 10, 23–26, 33, 38) (Fig. 7B).

SpoVID and SafA orthologs are present in all *Bacillus* species whose genomes have been sequenced to date, as well as in other related species (not shown). Importantly, the recent study of a SafA ortholog, called ExsA, revealed its role in promoting anchoring of both the coat and exosporium layers to the spore in *B. cereus* (1). Together with the observation that region A is highly conserved among SafA orthologs (Fig. 7A), this suggests that the overall role and perhaps some of the mechanistic details of the functioning of SafA in coat morphogenesis are conserved in the *Bacillus* group of spore formers.

ACKNOWLEDGMENTS

We thank Melissa Wilby (Emory University) for comments on the manuscript and John Pohl (Emory Microchemical Facility) for the mass spectrometry analysis.

This work was supported by European Union grant QLK5-CT-2001-01729 and by grant CONC-REEQ/692/2001 from "Fundação para a Ciência e a Tecnologia" (FCT) to A.O.H. and by NIH grant GM54395 to C.P.M. T.C. (SFRH/BD/1167/00) and A.L.I. (SFRH/BPD/8967/2002) were the recipients of fellowships from FCT.

REFERENCES

1. **Bailey-Smith, K., S. J. Todd, T. W. Southworth, J. Proctor, and A. Moir.** 2005. The ExsA protein of *Bacillus cereus* is required for assembly of coat and exosporium onto the spore surface. J. Bacteriol. **187:**3800–3806.

2. **Bateman, A., and M. Bycroft.** 2000. The structure of a LysM domain from *E. coli* membrane-bound lytic murein transglycosylase D (MltD). J. Mol. Biol. **299:**1113–1119.
3. **Bauer, T., S. Little, A. G. Stöver, and A. Driks.** 1999. Functional regions of the *Bacillus subtilis* spore coat morphogenetic protein CotE. J. Bacteriol. **181:**7043–7051.
4. **Beall, B., A. Driks, R. Losick, and C. P. Moran, Jr.** 1993. Cloning and characterization of a gene required for assembly of the *Bacillus subtilis* spore coat. J. Bacteriol. **175:**1705–1716.
5. **Birkeland, N. K.** 1994. Cloning, molecular characterization, and expression of the genes encoding the lytic functions of lactococcal bacteriophage phi LC3: a dual lysis system of modular design. Can. J. Microbiol. **40:**658–665.
6. **Bourne, N., P. C. FitzJames, and A. I. Aronson.** 1991. Structural and germination defects of *Bacillus subtilis* spores with altered contents of a spore coat protein. J. Bacteriol. **173:**6618–6625.
7. **Catalano, F. A., J. Meador-Parton, D. L. Popham, and A. Driks.** 2001. Amino acids in the *Bacillus subtilis* morphogenetic protein SpoIVA with roles in spore coat and cortex formation. J. Bacteriol. **183:**1645–1654.
8. **Costa, T., L. Steil, L. O. Martins, U. Völker, and A. O. Henriques.** 2004. Assembly of an oxalate decarboxylase produced under σ^K control into the *Bacillus subtilis* spore coat. J. Bacteriol. **186:**1462–1474.
9. **Cutting, S. M., and P. B. V. Horn.** 1990. Genetic analysis, p. 27–74. *In* C. R. Harwood and S. M. Cutting (ed.), Molecular biological methods for *Bacillus*. John Wiley & Sons Ltd., Chichester, England.
10. **Donovan, W., L. B. Zheng, K. Sandman, and R. Losick.** 1987. Genes encoding spore coat polypeptides from *Bacillus subtilis*. J. Mol. Biol. **196:**1–10.
11. **Driks, A.** 1999. *Bacillus subtilis* spore coat. Microbiol. Mol. Biol. Rev. **63:**1–20.
12. **Driks, A., S. Roels, B. Beall, C. P. Moran, Jr., and R. Losick.** 1994. Subcellular localization of proteins involved in the assembly of the spore coat of *Bacillus subtilis*. Genes Dev. **8:**234–244.
13. **Eichenberger, P., M. Fujita, S. T. Jensen, E. M. Conlon, D. Z. Rudner, S. T. Wang, C. Ferguson, K. Haga, T. Sato, J. S. Liu, and R. Losick.** 2004. The program of gene transcription for a single differentiating cell type during sporulation in *Bacillus subtilis*. PLoS Biol. **2:**e328.
14. **Henriques, A. O., B. W. Beall, and C. P. Moran, Jr.** 1997. CotM of *Bacillus subtilis*, a member of the alpha-crystallin family of stress proteins, is induced during development and participates in spore outer coat formation. J. Bacteriol. **179:**1887–1897.
15. **Henriques, A. O., B. W. Beall, K. Roland, and C. P. Moran, Jr.** 1995. Characterization of *cotJ*, a σ^E-controlled operon affecting the polypeptide composition of the coat of *Bacillus subtilis* spores. J. Bacteriol. **177:**3394–3406.
16. **Henriques, A. O., T. Costa, L. O. Martins, and R. Zilhão.** 2004. Functional architecture and assembly of the spore coat, p. 34–52. *In* E. Ricca, A. O. Henriques, and S. M. Cutting (ed.), Bacterial spores: probiotics and emerging applications. Horizon Scientific Press, London, United Kingdom.
17. **Henriques, A. O., L. R. Melsen, and C. P. Moran, Jr.** 1998. Involvement of superoxide dismutase in spore coat assembly in *Bacillus subtilis*. J. Bacteriol. **180:**2285–2291.
18. **Henriques, A. O., and C. P. Moran, Jr.** 2000. Structure and assembly of the bacterial endospore coat. Methods **20:**95–110.
19. **Itaya, M., K. Kondo, and T. Tanaka.** 1989. A neomycin resistance gene cassette selectable in a single copy state in the *Bacillus subtilis* chromosome. Nucleic Acids Res. **17:**4410.
20. **Joris, B., S. Englebert, C. P. Chu, R. Kariyama, L. Daneo-Moore, G. D. Shockman, and J. M. Ghuysen.** 1992. Modular design of the *Enterococcus hirae* muramidase-2 and *Streptococcus faecalis* autolysin. FEMS Microbiol. Lett. **70:**257–264.
21. **Kim, H., M. Hahn, P. Grabowski, D. C. McPherson, M. M. Otte, R. Wang, C. C. Ferguson, P. Eichenberger, and A. Driks.** 2006. The *Bacillus subtilis* spore coat protein interaction network. Mol. Microbiol. **59:**487–502.
22. **Klobutcher, L. A., K. Ragkousi, and P. Setlow.** 2006. The *Bacillus subtilis* spore coat provides "eat resistance" during phagocytic predation by the protozoan *Tetrahymena thermophila*. Proc. Natl. Acad. Sci. USA **103:**165–170.
23. **Kodama, T., H. Takamatsu, K. Asai, K. Kobayashi, N. Ogasawara, and K. Watabe.** 1999. The *Bacillus subtilis yaaH* gene is transcribed by SigE RNA polymerase during sporulation, and its product is involved in germination of spores. J. Bacteriol. **181:**4584–4591.
24. **Kodama, T., H. Takamatsu, K. Asai, N. Ogasawara, Y. Sadaie, and K. Watabe.** 2000. Synthesis and characterization of the spore proteins of *Bacillus subtilis*, YdhD, YkuD, and YkvP, which carry a motif conserved among cell wall binding proteins. J. Biochem. (Tokyo) **128:**655–663.
25. **Kuwana, R., Y. Kasahara, M. Fujibayashi, H. Takamatsu, N. Ogasawara, and K. Watabe.** 2002. Proteomics characterization of novel spore proteins of *Bacillus subtilis*. Microbiology **148:**3971–3982.
26. **Lai, E. M., N. D. Phadke, M. T. Kachman, R. Giorno, S. Vazquez, J. A. Vazquez, J. R. Maddock, and A. Driks.** 2003. Proteomic analysis of the spore coats of *Bacillus subtilis* and *Bacillus anthracis*. J. Bacteriol. **185:**1443–1454.
27. **Limpens, E., C. Franken, P. Smit, J. Willemse, T. Bisseling, and R. Geurts.** 2003. LysM domain receptor kinases regulating rhizobial Nod factor-induced infection. Science **302:**630–633.
28. **Little, S., and A. Driks.** 2001. Functional analysis of the *Bacillus subtilis* morphogenetic spore coat protein CotE. Mol. Microbiol. **42:**1107–1120.
29. **McPherson, D. C., H. Kim, M. Hahn, R. Wang, P. Grabowski, P. Eichenberger, and A. Driks.** 2005. Characterization of the *Bacillus subtilis* spore morphogenetic coat protein CotO. J. Bacteriol. **187:**8278–8290.
30. **Nicholson, W. L., and P. Setlow.** 1990. Sporulation, germination and outgrowth, p. 391–450. *In* C. R. Harwood and S. M. Cutting (ed.), Molecular biology methods for *Bacillus*. John Wiley & Sons Ltd., Chichester, England.
31. **Ozin, A. J., T. Costa, A. O. Henriques, and C. P. Moran, Jr.** 2001. Alternative translation initiation produces a short form of a spore coat protein in *Bacillus subtilis*. J. Bacteriol. **183:**2032–2040.
32. **Ozin, A. J., A. O. Henriques, H. Yi, and C. P. Moran, Jr.** 2000. Morphogenetic proteins SpoVID and SafA form a complex during assembly of the *Bacillus subtilis* spore coat. J. Bacteriol. **182:**1828–1833.
33. **Ozin, A. J., C. S. Samford, A. O. Henriques, and C. P. Moran, Jr.** 2001. SpoVID guides SafA to the spore coat in *Bacillus subtilis*. J. Bacteriol. **183:**3041–3049.
34. **Price, K. D., and R. Losick.** 1999. A four-dimensional view of assembly of a morphogenetic protein during sporulation in *Bacillus subtilis*. J. Bacteriol. **181:**781–790.
35. **Radutoiu, S., L. H. Madsen, E. B. Madsen, H. H. Felle, Y. Umehara, M. Gronlund, S. Sato, Y. Nakamura, S. Tabata, N. Sandal, and J. Stougaard.** 2003. Plant recognition of symbiotic bacteria requires two LysM receptor-like kinases. Nature **425:**585–592.
36. **Real, G., S. Autret, E. J. Harry, J. Errington, and A. O. Henriques.** 2005. Cell division protein DivIB influences the Spo0J/Soj system of chromosome segregation in *Bacillus subtilis*. Mol. Microbiol. **55:**349–367.
37. **Sacco, M., E. Ricca, R. Losick, and S. Cutting.** 1995. An additional GerE-controlled gene encoding an abundant spore coat protein from *Bacillus subtilis*. J. Bacteriol. **177:**372–377.
38. **Seyler, R. W., Jr., A. O. Henriques, A. J. Ozin, and C. P. Moran, Jr.** 1997. Assembly and interactions of *cotJ*-encoded proteins, constituents of the inner layers of the *Bacillus subtilis* spore coat. Mol. Microbiol. **25:**955–966.
39. **Steen, A., G. Buist, K. J. Leenhouts, M. El Khattabi, F. Grijpstra, A. L. Zomer, G. Venema, O. P. Kuipers, and J. Kok.** 2003. Cell wall attachment of a widely distributed peptidoglycan binding domain is hindered by cell wall constituents. J. Biol. Chem. **278:**23874–23881.
40. **Takamatsu, H., T. Kodama, T. Nakayama, and K. Watabe.** 1999. Characterization of the *yrbA* gene of *Bacillus subtilis*, involved in resistance and germination of spores. J. Bacteriol. **181:**4986–4994.
41. **Zheng, L. B., and R. Losick.** 1990. Cascade regulation of spore coat gene expression in *Bacillus subtilis*. J. Mol. Biol. **212:**645–660.
42. **Zilhão, R., R. Isticato, L. O. Martins, L. Steil, U. Völker, E. Ricca, C. P. Moran, Jr., and A. O. Henriques.** 2005. Assembly and function of a spore coat-associated transglutaminase of *Bacillus subtilis*. J. Bacteriol. **187:**7753–7764.
43. **Zilhão, R., M. Serrano, R. Isticato, E. Ricca, C. P. Moran, Jr., and A. O. Henriques.** 2004. Interactions among CotB, CotG, and CotH during assembly of the *Bacillus subtilis* spore coat. J. Bacteriol. **186:**1110–1119.